Controlling the disorder properties of quadratic nonlinear photonic crystals

Idith Varon,* Gil Porat, and Ady Arie

Department of Physical Electronics, Fleischman Faculty of Engineering, Tel Aviv University, Tel Aviv 69978, Israel

**Corresponding author: idithf@gmail.com*

Received July 5, 2011; accepted September 5, 2011;
posted September 12, 2011 (Doc. ID 150520); published October 5, 2011

We experimentally demonstrate a modulation scheme for disordered nonlinear crystals that combines periodic modulation and disordered sections. The crystal is divided into a set of identical periodically poled building blocks, whereby each block is followed by a short section of random length. We use this scheme to achieve broadband second harmonic generation in $KTiOPO_4$ nonlinear crystals while independently controlling the bandwidth and the center of the converted wavelengths as well as the efficiency of conversion. The trade-off between bandwidth and efficiency is improved in comparison with periodically poled crystals. © 2011 Optical Society of America

OCIS codes: 160.1245, 190.0190, 190.2620.

For many years, ordered nonlinear crystals, having either a homogeneous or periodically modulated second-order nonlinear coefficient, were considered the ideal medium for nonlinear optical processes. However, in recent years it has been shown that disordered nonlinear crystals [1,2] have some advantages with respect to ordered crystals—in particular, a significantly wider tolerance to phase mismatch owing to the variation in source wavelength, propagation angle, or crystal temperature. Disordered crystals can be produced naturally—for example using multidomain SBN crystals [1,3] or polycrystalline ZnSe [2]. Recently, electric field poling of ferroelectric crystals has been used for the same purpose—by either using highly dense gratings [4], or by utilizing a 2D or 1D mask with artificially designed disorder [5,6]. It was shown that these disordered crystals are useful for characterization of ultrashort pulses [3,7] and for generating higher harmonics by cascaded processes [8].

It is important to emphasize that the nonlinear coefficient of all these structures is not random—there is a short range (e.g., the domain size in SBN, the grain size of polycrystalline ZnSe) in which the value of the nonlinear coefficient is homogeneous, but over a larger range the values become uncorrelated. The total nonlinearly generated intensity mainly includes the separate contribution of each one of these ordered sections [9]. Therefore, the parameters of the ordered part in the disordered crystal determine the efficiency and bandwidth of the device. For example, it was shown that in case the ordered section is homogeneous, the optimal size is the coherence length of the nonlinear process [2], which is typically only a few micrometers. Because this section is so short, the generated wave in each ordered section is quite weak and the overall efficiency of the disordered device is low. Moreover, the spectral acceptance of this structure is determined by the length of the ordered section and cannot be independently optimized. In this Letter we propose a new scheme for designing disordered crystals, which completely removes the size limitations of the ordered part. Ordered sections of arbitrary length can be used, by combining periodic modulation and random segments. This scheme provides independent control of the acceptance bandwidth and conversion efficiency of the nonlinear process. Specifically, we utilize it to obtain better a trade-off between bandwidth and efficiency with respect to periodically poled crystals.

Figure 1 illustrates the proposed short range order (SRO) structure. It consists of identical periodic building blocks (BBs) in which the last domain is extended by a random length. In each BB, the nonlinear coefficient is periodically modulated at a period $\Lambda = 2\pi/\Delta k$, where Δk is the phase mismatch of second harmonic generation (SHG) of the central wavelength. The extensions are typically small in comparison with the BBs, so they can be regarded as the addition of a random phase to the SH field emanating from a periodically poled crystal of the BB's length.

As will be shown, the spectral bandwidth inversely depends on the length of the identical BBs (or equivalently, the number of domains per BB), while the efficiency depends on the total crystal length, so the two parameters can be controlled separately. If a periodically poled crystal of total length L is divided into N BBs separated by random domain extensions, while maintaining the total length L (i.e., the length of each BB is roughly L/N), the bandwidth would increase by N owing to the shorter length of each BB, while the efficiency would decrease by N as well [9]. In comparison, in order to increase the bandwidth in case of a periodically poled crystal by N, the interaction length must be shortened by N, but this would result in a loss in efficiency of N^2 times.

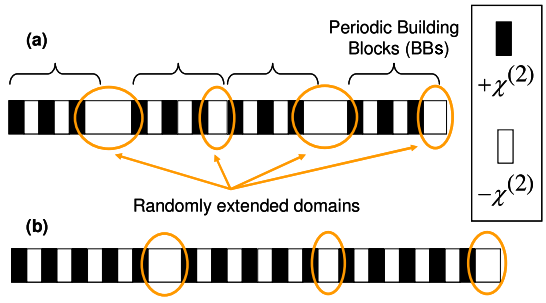

Fig. 1. (Color online) SRO structure, consisting of identical periodic BBs in which the last domain is extended by a random length: (a) 6 and (b) 10 domains per BB.

For a certain choice of design parameters, such as BB and crystal lengths, each realization of random extensions in the poling pattern produces a different spectral acceptance curve, with dips in efficiency at certain varying wavelengths. The width of the dips in efficiency is inversely proportional to the total crystal length. To obtain a relatively smooth curve with few dips, we can simulate different realizations and select the one that maximizes the figure of merit

$$\Gamma = \mathrm{FWHM} \times \frac{\mathrm{Avg}}{\mathrm{RMS}}, \tag{1}$$

where FWHM is the acceptance bandwidth of the crystal for a given pump linewidth and Avg and RMS are the average and root mean square of the SHG normalized efficiency ($I_{2\omega}/I_{\omega}^2$) within FWHM bounds. Γ is therefore maximized when the product of the average efficiency and acceptance bandwidth is optimized, while the dips in efficiency are kept to a minimum. Less optimal realizations result in a nonconstant response within FWHM bounds, even after the smoothing of the dips by the use of a broadband source, as will be later discussed.

We tested the design algorithm on a 15 mm long $KTiOPO_4$ (KTP) crystal. We chose four different SRO realizations, as depicted in Fig. 1, with a different number of domains per BB. Two of the four have the same BB length but different random extension realizations, one optimal according to the criterion described in Eq. (1) and the other suboptimal. These designs were then used to modulate the nonlinear coefficient of KTP by electric field poling. For comparison, we poled two additional periodic gratings on the crystal, a 15 mm long structure and a shorter 4.72 mm long structure. The period of the periodic sections is 27.7 μm, corresponding to a central phase-matched pump wavelength of 1650 nm.

An optical parametric oscillator (OPO) was used as a tunable pump, delivering 6 ns light pulses with a repetition rate of 10 kHz around a wavelength of 1650 nm. The input beam was weakly focused, and the waist diameter at the center of the sample was about 150 μm. Unless differently stated, the average (peak) power at the entrance of the crystal was kept constant at 5 mW (80 W).

The spectral width of the source was controlled by changing the input power to the OPO, which slightly modified the beam parameters, such as waist diameter and pulse duration from one measurement to another, within the same order of magnitude. In any case, results presented at the same source spectral width are kept under the same conditions.

Each point on the following curves shows the total SH power collected at the end of the crystal versus the central wavelength of the source. It therefore represents an averaging over a spectral window about as wide as the source, around each point, which smooths out the inherent dips in efficiency.

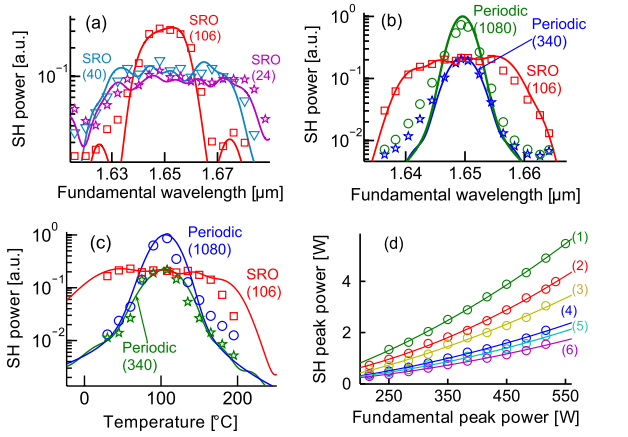

Fig. 2. (Color online) (a)–(c) Measured (dots) and calculated (lines) normalized SH power as function of central fundamental wavelength (a), (b) and as a function of temperature (c), for several SRO and periodic gratings. Number of domains per BB is stated in parentheses. (d) Measured (dots) SH peak power at different fundamental peak powers and second-order polynomial fits (lines) for each of the six gratings of the sample. From top to bottom: (1) 15 mm long periodic, (2) SRO with 106 domains per BB—optimal realization, (3) same with suboptimal realization, (4) 4.72 mm long periodic, (5) 40 domains per BB, and (6) 24 domains per BB. The central fundamental wavelength in (c), (d) is 1650 nm. The source linewidth is about 6.5 nm (a), 3 nm (b), (c) and 9 nm (d).

In simulations, the Sellmeier equation of [10,11] for bulk KTP at 125 °C was used to estimate the wavelength dependence of the refractive index. In experiment, however, the peak in efficiency was obtained at 108 °C [see Fig. 2(c)]; therefore, all presented measurements were taken at this temperature, and the simulated results were downshifted by 17 °C for comparison with the experiments. Simulations were performed with plane waves and under the undepleted pump approximation regime. The source was assumed to be of a Gaussian spectral shape around the central fundamental wavelength. The spectral width of the source was taken into account according to [12].

Figure 2(a) shows the measured and simulated SH power obtained with SROs of different BB lengths for a constant total length of 15 mm. The fewer domains there are per BB (which means that the BB is shorter), the broader the acceptance bandwidth at the expense of efficiency. The bandwidth of an SRO with 24 domains per BB was measured here to be about 55 nm.

Figure 2(b) shows a comparison between the 15 mm SRO grating divided into 10 periodic BBs, each consisting of 106 nonlinear domains and the two periodic gratings. The 4.72 (15) mm periodic structure can be regarded as a single BB structure with 340 (1080) domains. Note that the acceptance bandwidth of the SRO structure is about 3.5 times broader than that of the short periodically poled structure, while giving the same peak SH power.

Table 1. Normalized Efficiency

Grating	Periodic (1080)	SRO (106), Optimal Realization	SRO (106), Suboptimal Realization	Periodic (340)	SRO (40)	SRO (24)
Efficiency (%/W)	2.36E – 3	1.95E – 3	1.53E – 3	1.06E – 3	0.93E – 3	0.78E – 3

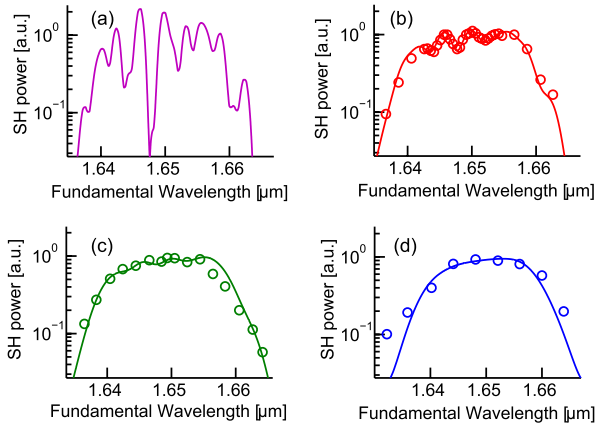

Fig. 3. (Color online) Measured (circles) and calculated (lines) SH power obtained by a 15 mm SRO crystal with 106 domains per BB with source linewidths of [(a), calculated only] 0, (b) 2.3, (c) 3, and (d) 6.5 nm. Power is individually normalized to make the curve shapes comparable.

A similar effect is observed when measuring the thermal acceptance bandwidth, as shown in Fig. 2(c).

In Fig. 2(d), we display the SH peak power for different fundamental peak powers at a fundamental wavelength of 1650 nm. The response is quadratic for all sample gratings. The normalized efficiency in %/W inside the crystal is shown in Table 1. In calculating the peak power from the average power obtained in experiment, the beam is assumed to have a Gaussian temporal profile. The Fresnel reflection from both facets of the crystal is taken under consideration in the calculated efficiency. It is quite clear that the efficiency of the SRO structures increases with the number of domains per BB.

Figure 3 demonstrates the effect of the spectral width of the source on the shape of the conversion acceptance curve. In the case of a monochromatic source [Fig. 3(a)], the amplitude of the dips in efficiency at certain wavelengths is greatest. When the source is narrow, the dips are apparent, while for an increasingly broader source bandwidth, their amplitude decreases. The response is ideal for a certain width of source corresponding to the typical width of the dips. When the source spectral width is comparable with the bandwidth of the crystal's acceptance curve for a monochromatic source, changing the modulation scheme or crystal length would hardly affect the resulting curve. In this case, shortening the length of a periodic crystal barely gains in bandwidth, while the SRO crystal still gives an advantage in this regard, as can be seen in Fig. 2(b).

In conclusion, we designed and fabricated a nonlinear crystal with several short range ordered gratings and have realized broadband SHG using a spectrally broad source. We obtained a better trade-off between bandwidth and efficiency than a periodically poled structure. We have demonstrated how the efficiency and bandwidth of light converted in SRO structures can be independently controlled through the choices of total crystal length and BB length, respectively. The concept of periodically poled BBs with random extensions can also be applied in two-dimensional nonlinear modulation, thereby enabling improvement of the trade-off between angular acceptance and efficiency [1]. Another possibility for both 1D and 2D structures is to use quasiperiodic modulation [13] inside the BBs, which can provide even wider spectral acceptance.

This work was supported by the Israel Science Foundation (ISF) through grant 774/09.

References

1. A. R. Tunyagi, M. Ulex, and K. Betzler, Phys. Rev. Lett. **90**, 243901 (2003).
2. M. Baudrier-Raybaut, R. Haïdar, Ph. Kupecek, Ph. Lemasson, and E. Rosencher, Nature **432**, 374 (2004).
3. R. Fischer, D. N. Neshev, S. M. Saltiel, A. A. Sukhorukov, W. Krolikowski, and Y. S. Kivshar, Appl. Phys. Lett. **91**, 031104 (2007).
4. S. Stivala, A. C. Busacca, A. Pasquazi, R. L. Oliveri, R. Morandotti, and G. Assanto, Opt. Lett. **35**, 363 (2010).
5. Y. Sheng, J. Dou, B. Ma, B. Cheng, and D. Zhang, Appl. Phys. Lett. **91**, 011101 (2007).
6. Y. Sheng, D. Ma, M. Ren, W. Chai, Z. Li, K. Koynov, and W. Krolikowski, Appl. Phys. Lett. **99**, 031108 (2011).
7. J. Trull, S. Saltiel, V. Roppo, C. Cojocaru, D. Dumay, W. Krolikowski, D. N. Neshev, R. Vilaseca, K. Staliunas, and Y. S. Kivshar, Appl. Phys. B **95**, 609 (2009).
8. Y. Sheng, S. M. Saltiel, and K. Koynov, Opt. Lett. **34**, 656 (2009).
9. A. Arie and N. Voloch, Laser Photon. Rev. **4**, 355 (2010).
10. K. Fradkin, A. Arie, A. Skliar, and G. Rosenman, Appl. Phys. Lett. **74**, 914 (1999).
11. S. Emanueli and A. Arie, Appl. Opt. **42**, 6661 (2003).
12. G. Imeshev, M. A. Arbore, and M. M. Fejer, J. Opt. Soc. Am. B **17**, 30 (2000).
13. R. Lifshitz, A. Arie, and A. Bahabad, Phys. Rev. Lett. **95**, 133901 (2005).